AMSTECS 2011, Tokyo, Japan
10-12 June 2011

DETECTING SOIL LAYER CONDITION SOON AFTER MERAPI ERUPTION 2010 USING ALOS/PALSAR DATA

Asep Saepuloh[1,3*], Krissandi Wijaya[2], Prihadi Sumintadireja[3]
[1]Advanced Industrial Science and Technology (AIST), Japan
[2]Jenderal Soedirman University (Unsoed), Indonesia
[3]Bandung Institute of Technology (ITB), Indonesia

*Corresponding author: saepuloh@gmail.com

ABSTRACT

Mt. Merapi located in the Central Java-Indonesia is the most active volcano over the world. The disaster usually occurs when the hot pyroclastic flows reached to the dense populated area around the volcano. The latest eruption in November 2010 caused fatalities to about 150 people died and 280.000 people sent to flee. The pyroclastic flow deposits reached about 15 km from the summit to the southern flank and devastated everything on their path. The eruption also caused significant change to the land cover around the volcano. This paper presents the effect of the hot pyroclastic flows and ashes to the soil layer condition soon after eruption. The purpose of this study is to quantify the damage level of the soil layer in accordance with soil moisture condition. The two scenes of Phased Array L-band type Synthetic Aperture Radar (PALSAR) onboard Advanced Land Observing Satellite (ALOS) were used in this study. The advantage of ALOS/PALSAR is that the sensor can penetrate vegetation canopy. Therefore, the soil layer could be identified clearly. The acquisition dates of the both data are before and after the eruption. Change detection analyses are applied to the two backscatter intensities of ALOS/PALSAR data. The hot pyroclastic flows decreased the backscatter intensity of soil layer about -15 dB. On the contrary, the ashes increased the backscatter intensity of soil layer about 12 dB. The damage levels are calculated by taking the cosine angle of the square root of the two backscatter intensities. The highest damage level was located at the main path of pyroclastic flow deposits. The medium damage level was located at the ashes deposits. The both damage levels might to be caused by the change of soil moisture and texture. This result could be used for delineating farming possibility area and/or disaster recovery after the eruption.

Keywords: Mt. Merapi, pyroclastics, PALSAR, soil moisture content

1. INTRODUCTION

Mapping of the soil layer in an active volcano usually needs extra cost and time, since the high slop of topography prevents the surveyor to reach the target. The remote sensing technology is proved effective to solve the problem due to capability of the sensor to detect spatially and temporally of wide area (e.g., Anderson et al., 2008; Tapiador and Casanova, 2003; Ma et al., 2004). However, the application of remote sensing technology in the Torrid Zone such as Indonesia is still limited because the clouds and vegetation always cover the target area (Saepuloh et al., 2010). Moreover, the hazard from the volcano also contributes to the difficulties of mapping activities. This paper presents a new developed application to overcome such the problem using the Phased Array L-band type Synthetic Aperture Radar (PALSAR).

Mt. Merapi located in Central Java, Indonesia is selected as study area (see Fig. 1). This volcano is the most suitable for this study because it has a high activity, which usually affects to the urban area. The latest eruption in November 2010 is used as the case study in this paper. This eruption period is the strongest eruption during the last fifteen years. Therefore, the soil layer around the volcano might be affected strongly.

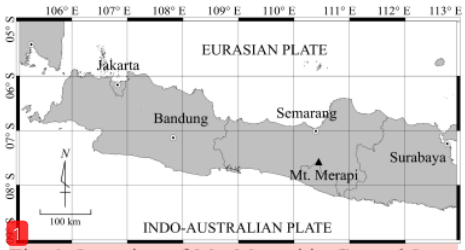

Fig. 1. Location of Mt. Merapi in Central Java, Indonesia.

Four scenes of ALOS/PALSAR data in this study are listed in Table 1. Regarding to the tracking of the satellite, there are two types of the data: descending and ascending. The descending mode is the track of satellite from North to the South Pole with looking sensor to the left. On the contrary, the ascending mode indicates the satellite track from South to North Pole with right looking sensor. The descending mode was used to extract the coverage area of the pyroclastic flow and ash fall deposits termed as PF and AF, respectively. Meanwhile, the ascending mode was used to calculate the damage level of the soil layers which is affected by the PF and AF.

Table 1. Data used in this study.

No	Acquisition date	Path	Row	Mode
1	Sept. 12, 2007	93	378	descending
2	Nov. 5, 2010	93	378	descending
3	Sept. 16, 2010	431	703	ascending
4	Nov. 1, 2010	431	703	ascending

2. BACKSCATTERING INTENSTIES TO DELINEATE DAMAGE AREA

The ALOS/PALSAR is similar with the other Synthetic Aperture Radar (SAR) sensor in which the data is composed by complex number. The magnitude can be extracted from the complex data by taking the square root of power of the real and imaginary part. The magnitude is presented by digital number (*DN*) in the image. Therefore, the backscatter intensity can be defined simply as:

$$\beta = 10 \times log(DN)\ \text{dB} \qquad (1)$$

The unit of β is decibel (dB) due to logarithmic scale of the *DN*.

Fig. 2 shows the two β images with acquisition dates are before and after the eruption in November 2010. The gray level scale presents the β value in dB. Dark tones indicated low backscatter return to the receiver caused by flat slop, smooth, or low moisture of material at the surface. On the contrary, bright tones indicated high backscatter return to the receiver. The different tones in the images were caused by slope, roughness, and/or dielectric constant of material at the surface. High slope aligned to the sensor caused the β brighter than flat slope. By taking the ratio of the two β data, the slope effect can be reduced. The roughness and dielectric constant of material at surface are still influence in the image. Therefore, the detection is focused on soil moisture and texture (SMT) as a portion of dielectric constant and roughness.

Fig. 2A shows that the dark tones are located at the west from the summit. Fig. 2B shows that the dark tones expanded to the West and South. The expansion of the dark tones was caused by the change of the soil layer characteristics after the eruption. In addition, the bright tones are also located at the Southern part from the summit (see Fig. 2B). Therefore, the PF and AF changed the β value to be lower and higher than before the eruption, respectively.

Fig. 3 shows the ratio of β images. The magenta and cyan portion indicated strong changes in β image. Regarding the field observation, the magenta portions are the area which is devastated by PF. On the other hand, the cyan portion is the distribution of the AF.

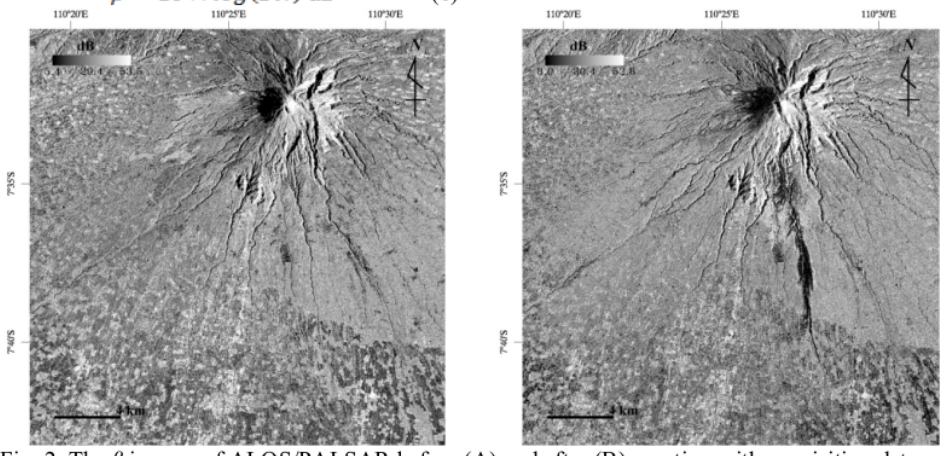

Fig. 2. The β images of ALOS/PALSAR before (A) and after (B) eruption with acquisition dates are depicted by no. 1 and 2 in Table 1

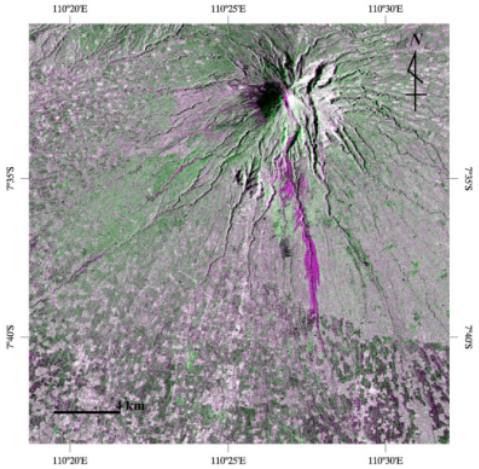

Fig. 3. The ratio of β overlaid on intensity image of ALOS/PALSAR.

The PF in massive magenta portion was distributed to the Southern flank from the summit. The calculated travel distance is about 16 km. The PF was also distributed to the western flank with travel distance about 8 km. Meanwhile, the distribution area of the AF is wider than PF. The ashes were ejected to the air by the high pressure of the eruption, then its fall to the ground by gravitational energy. Therefore, the ashes cover to almost all directions.

The PF and AF have changed the soil layer condition. To quantify the change, the base statistics were calculated for β image after the eruption (see Fig. 4). The mean of β for PF (about 19 dB) is lower than that for AF (about 25 dB). The standard deviation of PF is also lower than that of AF, indicating the variability of β value of PF is low.

Since the ALOS/PALSAR utilized in the L-band (a wavelength about 23.6 cm), the scattering measurements could estimate the surface (top 0-5 cm layer) soil moisture (Wang et al., 1989).

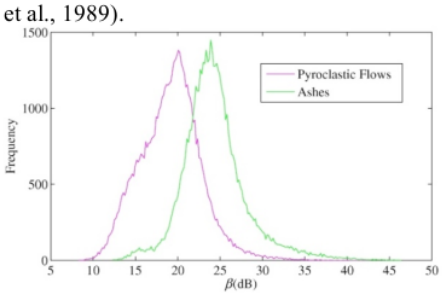

Fig. 4. The histogram of pyroclastic flows and ashes in β image of after eruption.

The soil moisture is a physical properties, in which can be detected by the SAR sensor as dielectric constant. Therefore, the damage area is described as the area where the SMT have been changed before to after the eruption.

The physical properties of soils at the field are varied, both in vertical and horizontal directions (Wijaya et al., 2004). Therefore, the damage area is described above is in horizontal and vertical meaning. The effect of AF and PF to the β is different. The AF increased the β of soil layer about 12 dB. On the contrary, the PF decreased the β of soil layer about -15 dB. The change of the β is supposed to be strongly related to the change in the SMT (Stroosnijder et al., 1986, Low et al., 2005). The AF increased the SMT, but the PF decreased the SMT. The decrease of the SMT is expected due to the burning effect from the hot PF. The water moisture in the soil was evaporated to the air after the devastation took place. On the other hand, the AF increased the SMT might be because of the infiltration of the meteoric water to the ejected-ash on the air (Textor et al., 2006). In addition, this also might be encouraged by the high water retention of the mixed fine ash-top soil layer to the prolonged rainfall soon after the eruption (Shoji, 1993).

3. DETECTING DAMAGE LEVEL OF SOIL LAYER

Since the L-band has capability to penetrate the soil layer, this data can be used to quantify the damage level of the soil in accordance to the change of the SMT. The damage level δ is defined by:

$$\delta = \cos^{-1}\left(\frac{\sum_{w=1}^{W}\beta_1 \times \beta_2}{\sqrt{\sum_{w=1}^{W}\beta_1^2 \times \sum_{w=1}^{W}\beta_2^2}}\right) \qquad (2)$$

Where the W is a window size of estimated target area in pixel, w is starting count of the W, β_1 and β_2 are backscatter intensities of data 1 and 2, respectively. An iterative method was used to calculate the δ for the entire pixel in the image. The purpose of taking the cosine function is to obtain the ascent value as increase of damage level.

Fig. 5 shows the damage level map of the SMT. The color bar indicated the increasing level from blue to red. The strongest damages are located around the summit as depicted by red color. The massive damages are also located at the main path of the PF as described in Fig. 3.

The medium damages are located at the distribution area of the AF in green portion. The damage area by the AF is wider than PF due to air ejection from the eruption. The low damages is depicted by blue portion indicated that the SMT is not affected strongly by the eruption. Overall it can be observed that the PF had stronger effect on the SMT than the AF.

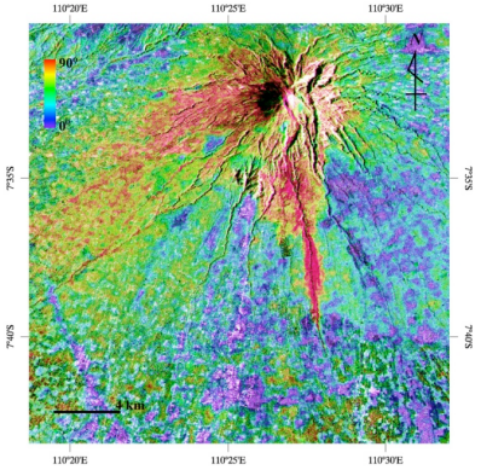

Fig. 5. The damage level map of soil layer calculated from the cosine angle of the ratio of the two β data.

4. CONCLUSION

The distribution area as well as short-term effect of the PF and AF from the currently erupted Mt. Merapi (November 2010) on soil layer condition was successfully identified through the remote sensing analysis. The PF resulted in lowering the β value up to -15 dB that reflected the low SMT. On the other hand, the AF increased the β value up to 12 dB that related to the high SMT. Both phenomena were due to the PF burning effect on the soil surface and the meteoric water absorption by the volcanic ash particles, respectively. The high water retention of the mixed fine ash-top soil layer to the prolonged rainfall soon after the eruption might also caused the latter.

The damage level of soil layer was determined based the β values that are strongly corresponded to the SMT. The highest damage level was located at surrounding the summit area and at the main path of PF deposits, while the medium damage level was located at the AF deposits. The damage area by the AF was wider than PF due to air ejection from the eruption.

REFERENCES

[1] **Anderson MC, Norman JM, Kustas WP, Houborg R, Starks PJ, Agam N** (2008) A Thermal-Based Remote Sensing Technique for Routine Mapping of Land-Surface Carbon, Water and Energy Fluxes From Field To Regional Scales. *Remote Sensing of Environment* 112:4227-4241.

[2] **Low A , Ludwig R, Mauser W** (2005) Use of microwave remote sensing data to monitor spatio temporal characteristics of surface soil moisture at local and regional scales. *Advance in Geosciences* 5: 49-56.

[3] **Ma Y, Menenti M, Tsukamoto O, Ishikawa H, Wang J, Gao Q** (2004) Remote sensing parameterization of regional land surface heat fluxes over arid area in northwestern China. *Journal of Arid Environments* 57:257-273.

[4] **Shoji, S** (1993) Studies on early weathering of volcanic ash and rehabilitation of soil environment. Report No. 04453126 for the Grant-in-Aid of Scientific Research from the Ministry of Education.

[5] **Saepuloh A, Koike K, Omura M, Iguchi M, Setiawan A** (2010) SAR- and gravity change-based characterization of the distribution pattern of pyroclastic flow deposits at Mt. Merapi during the past 10 years. *Bulletin of Volcanology* 72: 221-232.

[6] **Stroosnijder L, Lascano RJ, Van Bavel CHM, Newton RW** (1986) Relation between l-band soil emittance and soil water content. *Remote Sensing of Environment* 19:117-125.

[7] **Tapiador FJ, Casanova JL** (2003) Land use mapping methodology using remote sensing for the regional planning directives in Segovia, Spain. *Landscape and Urban Planning* 62:103-115.

[8] **Textor C, Graf HF, Herzog M, Oberhuber JM, Rose WI, Ernst GGJ** (2006) Volcanic particle aggregation in explosive eruption columns. *JVGR* 150:359–377.

[9] **Wang JR, Shiue JC, Schmugge TJ, Engman ET** (1989) Mapping Surface Soil Moisture with L-Band Radiometric Measurements. *Remote Sensing of Environment* 27:305-312.

[10] **Wijaya K, Nishimura T, Kato M, Nakagawa M** (2004) Field Estimation of Soil Dry Bulk Density Using Amplitude Domain Reflectometry Data. *Journal of the Japanese Society of Soil Physics* 97:3-12.

10. Effect of organic fertilizer and application of charcoal on quality of potato tuber variety atlantic

ORIGINALITY REPORT

3%	3%	2%	0%
SIMILARITY INDEX	INTERNET SOURCES	PUBLICATIONS	STUDENT PAPERS

PRIMARY SOURCES

1	unit.aist.go.jp Internet Source	3%

Exclude quotes	On	Exclude matches	< 2%
Exclude bibliography	On		